

# The Relationship Between $^{13}\text{CO}/\text{C}^{18}\text{O}$ and Star Formation Rate Surface Density

Marz Newman<sup>1</sup> and Amanda Kepley<sup>2</sup>

<sup>1</sup>*Department of Physics & Astronomy, Louisiana State University, Baton Rouge, LA 70803, USA*

<sup>2</sup>*National Radio Astronomy Observatory, 520 Edgemont Road, Charlottesville, VA 22903, USA*

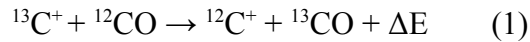
## ABSTRACT

Optically thin  $^{13}\text{CO}$  and  $\text{C}^{18}\text{O}$  allow us to investigate the physical causes for abundance variations across the spiral disks. Correlation between the  $^{13}\text{CO}/\text{C}^{18}\text{O}$  ratio and  $\Sigma_{\text{SFR}}$  can indicate either chemical fractionation or selective enrichment by stellar nucleosynthesis. We use data taken by the GBT and Argus to measure the  $^{13}\text{CO}/\text{C}^{18}\text{O}$  ratio and a combination of IR and far ultraviolet to trace star formation rate surface density ( $\Sigma_{\text{SFR}}$ ) in nearby spiral galaxies. This paper uses three different region selection methods to find the relation: the central  $15''$  of each galaxy,  $0.16 \times r_{25}$  of each galaxy, and radial profiles starting from the center and increasing by  $15''$  galactocentric radius for each region. After plotting the  $^{13}\text{CO}/\text{C}^{18}\text{O}$  ratio as a function of  $\Sigma_{\text{SFR}}$  for all region selection methods, we found that the  $^{13}\text{CO}/\text{C}^{18}\text{O}$  ratio increased with increasing  $\Sigma_{\text{SFR}}$  with a slope of  $0.07 \pm 0.03$  for central regions, decreased with increasing  $\Sigma_{\text{SFR}}$  with a slope of  $-0.7 \pm 1.0$  for whole galaxy regions, and consistently decreased for the radial profiles with two galaxies (NGC 3631 and NGC 5055) as outliers. We see evidence for both chemical fractionation and selective enrichment, indicating that no one mechanism appears to dominate in all scenarios.

## 1. INTRODUCTION

CO isotopologues are used as tracers of dense molecular gas and can help in the study of giant molecular clouds (GMCs), where star formation occurs.  $^{13}\text{CO}$  and  $\text{C}^{18}\text{O}$  are more effective at mapping inside dense molecular clouds than  $^{12}\text{CO}$  because they are optically thin while  $^{12}\text{CO}$  is optically thick. The  $^{13}\text{CO}/\text{C}^{18}\text{O}$  ratio allows for the tracing of abundance variations across the disks of galaxies. Changes in relative abundance between  $^{13}\text{CO}$  and  $\text{C}^{18}\text{O}$  could be caused by either abundance variations or changes in optical depth. Previous works have investigated the possibility that the variations in measurements of the  $^{13}\text{CO}/\text{C}^{18}\text{O}$  ratio are due to changes in optical depth (e.g. Jiménez-Donaire et al. 2017; Davis 2012). However, Jiménez-Donaire et al. found that  $^{13}\text{CO}$  was consistently optically thin, so this paper will focus on abundance variations rather than changes in optical depth.

There are two main physical causes for these abundance variations in  $^{13}\text{CO}$  and  $\text{C}^{18}\text{O}$ : chemical fractionation and stellar nucleosynthesis. Isotope dependent fractionation occurs in cold regions of galaxies and gives preferential formation to  $^{13}\text{CO}$  by the following formula:



The temperature in a region is proportional to  $\Sigma_{\text{SFR}}$ , so the amount of  $^{13}\text{CO}$  would decrease relative to  $\text{C}^{18}\text{O}$  as  $\Sigma_{\text{SFR}}$  increases, leading to a negative trend (e.g. Jiménez-Donaire et al. 2017).

Another phenomenon that could affect the relative abundance of the  $^{13}\text{CO}$  and  $\text{C}^{18}\text{O}$  molecules is selective enrichment by stellar nucleosynthesis.  $^{18}\text{O}$  is produced by high-mass stars while  $^{13}\text{C}$  is produced by intermediate-mass stars during the Helium Burning stage of their lives. High-mass star explosions would enrich the interstellar medium (ISM) with  $^{18}\text{O}$  on a short timescale, while intermediate-mass stars would emit  $^{13}\text{C}$  on a longer timescale (e.g. Jiménez-Donaire et al. 2017). Therefore, we expect the  $^{13}\text{CO}/\text{C}^{18}\text{O}$  ratio to be impacted by the ratio of high-mass to intermediate-mass stars, as well as the age of the stars in the region. A higher population of high-mass stars relative to intermediate-mass stars would cause a lower  $^{13}\text{CO}/\text{C}^{18}\text{O}$  ratio and recent star formation would also lower the  $^{13}\text{CO}/\text{C}^{18}\text{O}$  ratio due to the shorter timescale. Therefore, a positive or zero slope could be explained by older star populations with stellar nucleosynthesis.

In this paper, we use DEGAS data taken by the GBT and Argus to measure the  $^{13}\text{CO}/\text{C}^{18}\text{O}$  ratio as a function of star formation rate surface density (derived from IR and far ultraviolet data) for 15 nearby galaxies. We find the trends for three different region selection methods and identify the dominant abundance variation effect in each case.

## 2. METHODS

### 2.1 Region Selection

We use three different region selection methods to find the  $^{13}\text{CO}/\text{C}^{18}\text{O}$  ratio trend as a function of  $\Sigma_{\text{SFR}}$ —the central  $15''$  of each galaxy,  $0.16 \times r_{25}$  of each galaxy, and radial profiles starting from the center and increasing by  $15''$  galactocentric radius for each region. Shown in Figure 1 are examples of each region selection.

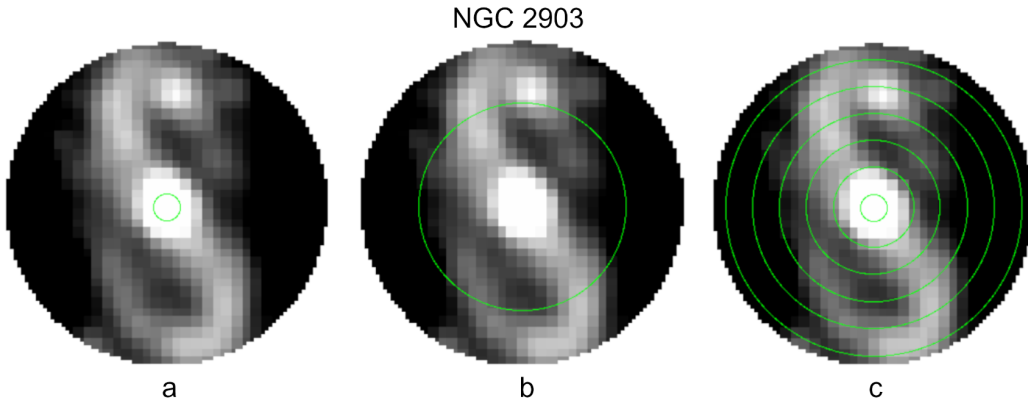


Fig. 1.— Depiction of the three types of region selections used in this paper with galaxy NGC 2903 as the example. Left: Central region with a diameter of  $15''$ . Middle: “Whole” galaxy region, with a radius of  $0.16 \times r_{25}$ . Right: Radial profile regions, starting with the central region and increasing by  $15''$  radius for each region.

Central regions for each galaxy were chosen to have a diameter of  $15''$  to be consistent with the resolution of the data. Regions that are 16% of the effective radius ( $r_{25}$ ) were chosen in order to encompass the largest area in all galaxies without exceeding the bounds of the observed area.

They will be referred to as whole galaxy regions throughout this paper. Radial profile regions begin with the central region and increase by 15'' radius for each region.

## 2.2 $^{13}\text{CO}/\text{C}^{18}\text{O}$ Ratio Calculations

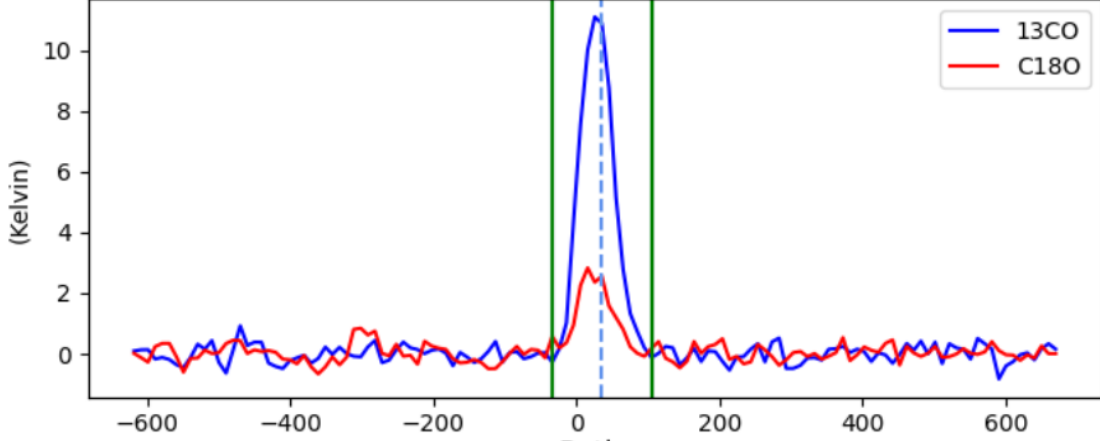


Fig. 2.— Spectra of  $^{13}\text{CO}$  (blue) and  $\text{C}^{18}\text{O}$  (red) used to find the ratio for galaxy IC 0342. The dotted blue line is the peak of  $^{13}\text{CO}$  and the vertical green lines show the range of the peak.

Star formation rate surface densities were calculated using a combination of IR and far ultraviolet data. To calculate the  $^{13}\text{CO}/\text{C}^{18}\text{O}$  ratio, we find the peak of  $^{13}\text{CO}$  in a spectra (e.g. Figure 2) and define a range containing the peaks of the molecules. The  $^{13}\text{CO}$  peak is used instead of the  $\text{C}^{18}\text{O}$  peak because  $^{13}\text{CO}$  consistently has a higher signal-to-noise ratio. We then find the sum of points within the range for both molecules and use these sums to calculate the ratio. The error in the  $^{13}\text{CO}$  and  $\text{C}^{18}\text{O}$  data points were found using the standard deviation of the first 40 channels. These errors were propagated to find the error of the ratio.

## 3. RESULTS

### 3.1 Center and Whole Galaxy Regions

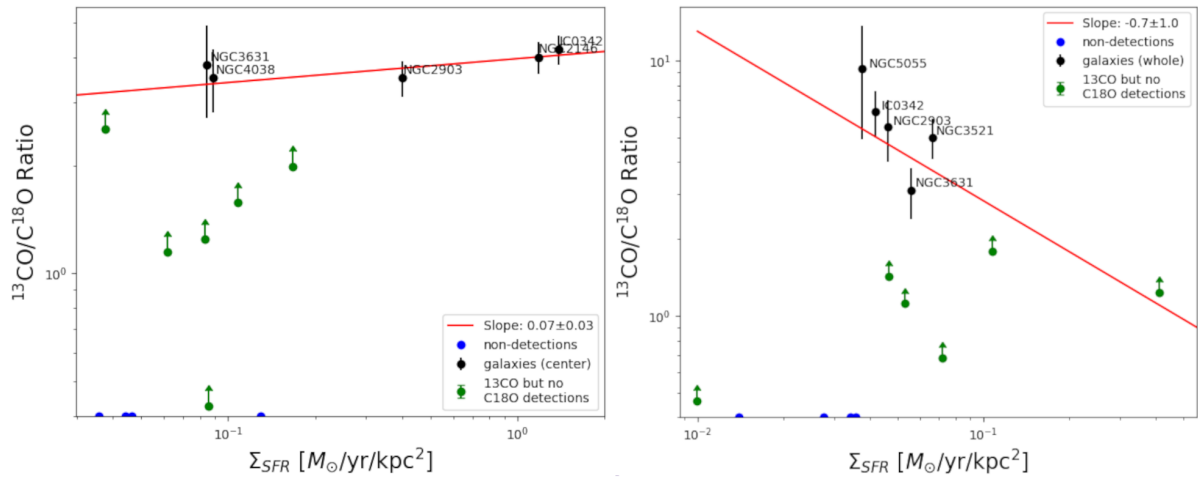


Fig. 3.— Plots of the  $^{13}\text{CO}/\text{C}^{18}\text{O}$  ratio as a function of  $\Sigma_{\text{SFR}}$  for center (left) and whole (right) galaxy regions, including detections in both  $^{13}\text{CO}$  and  $\text{C}^{18}\text{O}$  (black), detections in  $^{13}\text{CO}$  with non-detections in  $\text{C}^{18}\text{O}$  (green), and non-detections in both  $^{13}\text{CO}$  and  $\text{C}^{18}\text{O}$  (blue). Limits in green were found using  $3\sigma_{18}$ , where  $\sigma_{18}$  is the standard deviation of  $\text{C}^{18}\text{O}$  data. We use only the points with both  $^{13}\text{CO}$  and  $\text{C}^{18}\text{O}$  to find a line of best fit, shown in red.

Figure 3 shows the results of using central and whole regions to find the  $^{13}\text{CO}/\text{C}^{18}\text{O}$  ratio as a function of  $\Sigma_{\text{SFR}}$ . The whole galaxy plot has a slope of  $-0.7 \pm 1.0$  which would be consistent with either a negative or zero slope. The central regions plot has a slope of  $0.07 \pm 0.03$ . The apparent negative slope of the whole galaxy plot could be caused by chemical fractionation and the positive slope in the central regions plot would be explained by an older star population in the stellar nucleosynthesis scenario.

### 3.2 Radial Profiles

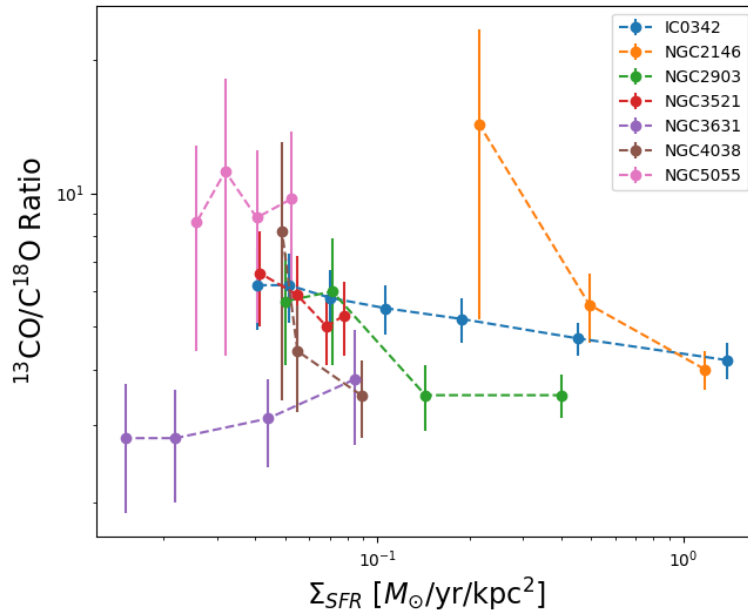


Fig. 4.— Radial profiles of galaxies with detections in both molecules, excluding lower limits. Each galaxy is indicated by a different color. From left to right, the points represent decreasing galactocentric radius, with the rightmost point being the closest to the center.

Figure 4 shows the radial profiles of each galaxy (separate plots of radial profiles can be found in Appendix A). The galaxies used for radial profiles are galaxies where detections were found in both  $^{13}\text{CO}$  and  $\text{C}^{18}\text{O}$  (black data points in Figure 3). Five of the seven galaxies show negative trends. NGC 3631 and NGC 5055 are outliers, where NGC 3631 has a slope of  $0.17 \pm 0.05$  and NGC 5055 has a slope of  $0.1 \pm 0.2$ . The slope of NGC 5055 is consistent with a slope of zero, but both of these outliers could be examples of stellar nucleosynthesis effects with older populations of stars.

#### 4. DISCUSSION

In order to explain the trends found in section 3, we look at two possible causes of changes in relative abundance between  $^{13}\text{CO}$  and  $\text{C}^{18}\text{O}$ . The scenarios we consider are isotope dependent fractionation and selective enrichment by stellar nucleosynthesis.

A previous publication found a negative correlation for the radial profiles of four galaxies, with one galaxy, NGC 628, showing a mostly positive trend as an outlier (Jiménez-Donaire et al. 2017). Another publication found no correlation between  $^{13}\text{CO}/\text{C}^{18}\text{O}$  ratio and  $\Sigma_{\text{SFR}}$  when using either galaxy centers or whole galaxy data for each spiral (Davis 2012).

Isotope dependent fractionation would explain the negative correlations we see in the majority of radial profiles as well as the whole galaxy regions in Figure 3, however it does not explain the positive slope seen in the central regions plot in Figure 3 or the two radial profile outliers, NGC 3631 and NGC 5055. We require an additional explanation for these observations.

Selective enrichment can explain the non-negative correlations we observe in Figure 3 and Figure 4. The outlier galaxy centers could include higher populations of intermediate-mass red giants or older star populations which would explain the apparent increase in  $^{13}\text{CO}$  relative to  $\text{C}^{18}\text{O}$ .

In this paper, we find evidence for both isotope dependent fractionation and stellar nucleosynthesis effects in our data. We can conclude that the correlation between the  $^{13}\text{CO}/\text{C}^{18}\text{O}$  ratio and  $\Sigma_{\text{SFR}}$  is dependent on one of these two physical effects for each galaxy and region selection.

Several data points this paper reports are lower limits caused by non-detections in  $\text{C}^{18}\text{O}$ . With better data, we could reduce the number of lower limits in this data set and include those points in the fit for more accurate results as possible future work.

#### 5. CONCLUSIONS

We report observations of the  $^{13}\text{CO}/\text{C}^{18}\text{O}$  ratio as a function of star formation rate surface density in nearby galaxies using data taken by the GBT and Argus. This paper uses three different region selection methods: central regions, whole galaxy regions, and radial profiles. We find that while the majority of radial profiles of the galaxies show negative correlations in Figure 4, there are a few examples of non-negative slopes in both the radial profiles and central regions ( $0.07 \pm 0.03$ ) in Figure 3. The slope of the whole galaxy regions plot ( $-0.7 \pm 1.0$ ) in Figure 3 is consistent with either a positive or zero slope.

In order to explain the results we find, we propose two physical phenomena as the causes for these abundance variations: chemical fractionation and stellar nucleosynthesis. A combination of these two scenarios could explain the differing trends we see in our data.

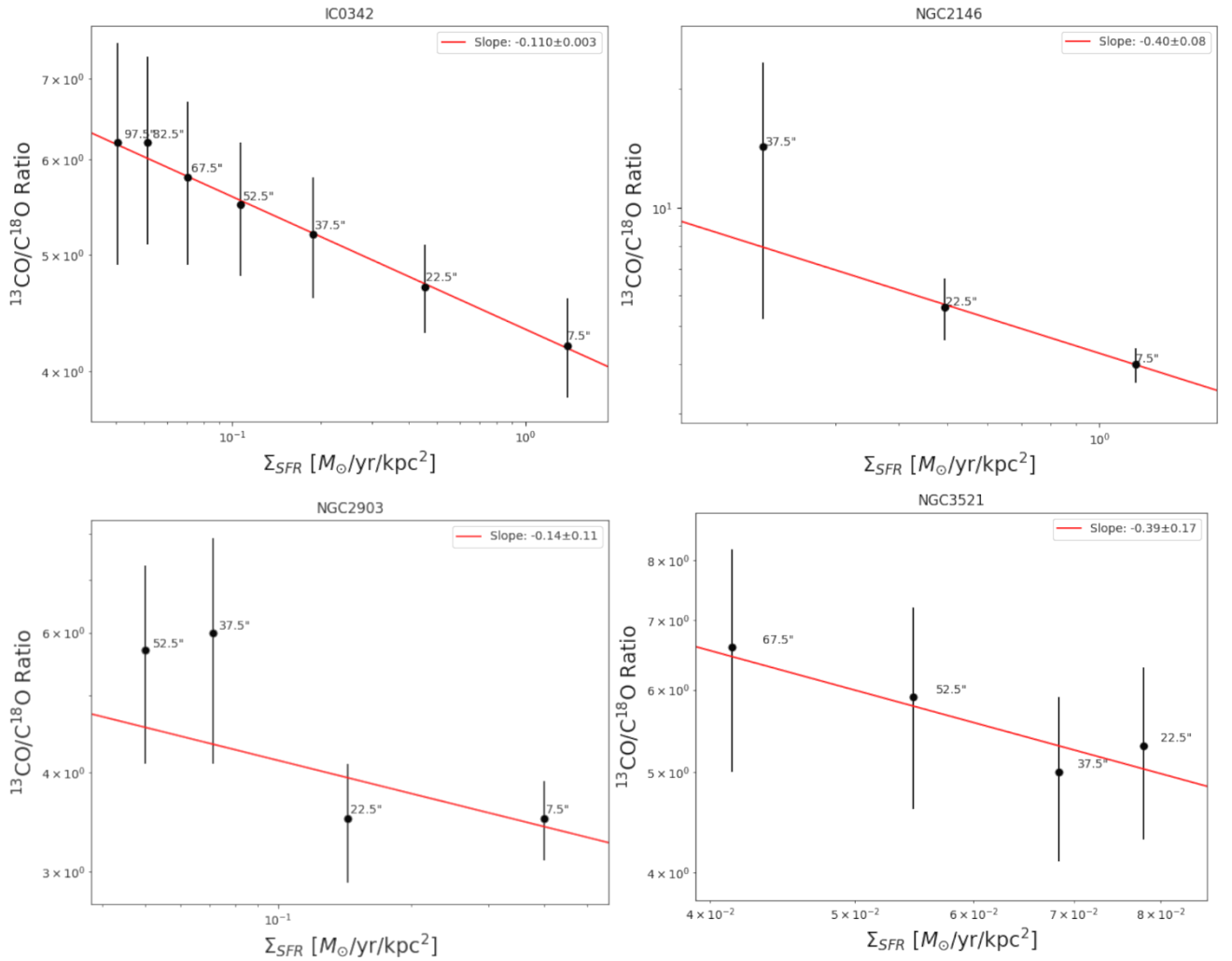
The Green Bank Observatory is a facility of the National Science Foundation operated under cooperative agreement by Associated Universities, Inc. The National Radio Astronomy Observatory is a facility of the National Science Foundation operated under cooperative agreement by Associated Universities, Inc. This publication makes use of data products from the

Wide-field Infrared Survey Explorer, which is a joint project of the University of California, Los Angeles, and the Jet Propulsion Laboratory/California Institute of Technology, funded by the National Aeronautics and Space Administration.

## REFERENCES

- Davis, Timothy A., 2012. Systematic variation of the  $^{12}\text{CO}/^{13}\text{CO}$  ratio as a function of star-formation rate surface density.
- Jiménez-Donaire, María et al., 2017.  $^{13}\text{CO}/\text{C}^{18}\text{O}$  gradients across the disks of nearby spiral galaxies. ApJ.

## APPENDIX A: RADIAL PROFILES



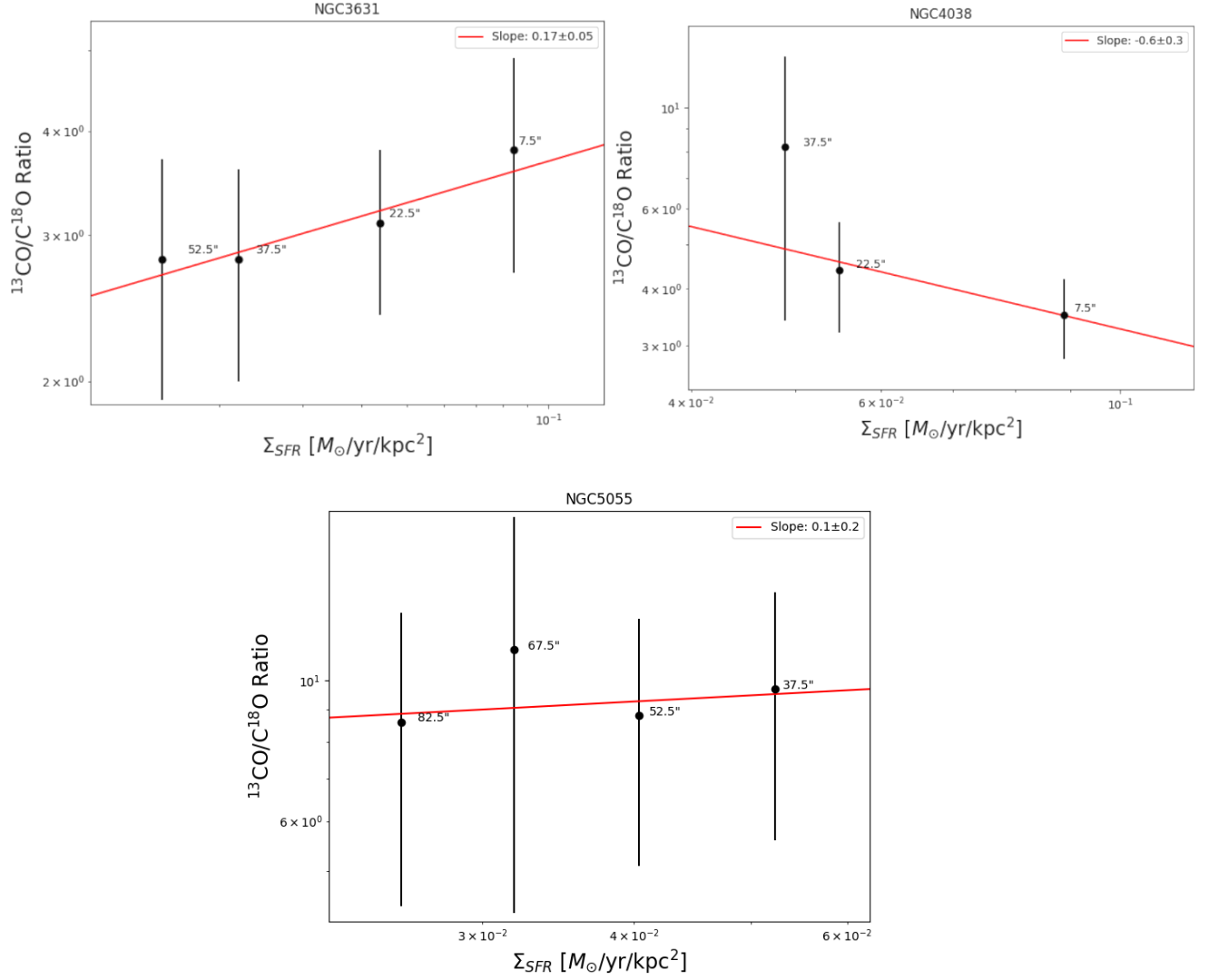


Fig. A1. — Radial profiles of the seven galaxies that had both  $^{13}\text{CO}$  and  $\text{C}^{18}\text{O}$  detections in Figure 3. Lower limits are not shown. Data points are labeled with the radius of the region used in arcseconds. The fit line is shown in red.